Hyperuniformity variation with quasicrystal local isomorphism class

2017 J. Phys.: Condens. Matter 29 204003

(http://iopscience.iop.org/0953-8984/29/20/204003)

IOP Publishing Journal of Physics: Condensed Matter
J. Phys.: Condens. Matter **29** (2017) 204003 (7pp) https://doi.org/10.1088/1361-648X/aa6944

Hyperuniformity variation with quasicrystal local isomorphism class

C Lin[1], P J Steinhardt[1,2] and S Torquato[1,2,3,4,5]

[1] Department of Physics, Princeton University, Princeton, NJ 08544, United States of America
[2] Princeton Center for Theoretical Science, Princeton University, Princeton, NJ 08544, United States of America
[3] Department of Chemistry, Princeton University, Princeton, NJ 08544, United States of America
[4] Program of Applied and Computational Mathematics, Princeton University, Princeton, NJ 08544, United States of America
[5] Princeton Institute for the Science and Technology of Materials, Princeton University, Princeton, NJ 08544, United States of America

E-mail: chaneyl@princeton.edu, steinh@princeton.edu and torquato@princeton.edu

Received 6 March 2017, revised 21 March 2017
Accepted for publication 27 March 2017
Published 13 April 2017

Abstract

Hyperuniformity is the suppression of long-wavelength density fluctuations, relative to typical structurally disordered systems. In this paper, we examine how the degree of hyperuniformity [$\overline{\Lambda}(\infty)$] in quasicrystals depends on the local isomorphism class. By studying the continuum of pentagonal quasicrystal tilings obtained by direct projection from a five-dimensional hypercubic lattice, we find that $\overline{\Lambda}(\infty)$ is dominantly determined by the local distribution of vertex environments (e.g. as measured by Voronoi cells) but also exhibits a non-negligible dependence on the restorability. We show that the highest degree of hyperuniformity [smallest $\overline{\Lambda}(\infty)$] corresponds to the Penrose local isomorphism class. The difference in the degree of hyperuniformity is expected to affect physical characteristics, such as transport properties.

Keywords: quasicrystals, hyperuniformity, local isomorphism class, Penrose tiling, restorability

(Some figures may appear in colour only in the online journal)

1. Introduction

There are uncountably many, physically distinct quasicrystals, which have the same symmetry, same fundamental repeating units (e.g. tiles, clusters of atoms or molecules), and same support for their diffraction patterns, but which have different space-filling arrangements of the repeating units and different peak intensities for their diffraction patterns [1–4]. These distinct quasicrystals are said to belong to different *local isomorphism* (LI) *classes*. All quasicrystals—and hence all LI classes—have long-wavelength density fluctuations that, like crystals and special amorphous systems, are suppressed relative to typical structurally disordered systems; this large-scale structural property is known as *hyperuniformity* [5–7]. Whether the degree of hyperuniformity, as measured by the leading coefficient of the number variance (defined below), varies with LI class is an open question. If it does vary, then it would be of interest to understand, first, what specific structural properties of an LI class determine the degree of hyperuniformity and, second, how these structural properties affect the physical properties.

On one hand, one might think the degree of hyperuniformity would not vary with LI class, given what different LI classes have in common, including how similar they are in their construction. With the direct projection method, different LI classes can be generated using an acceptance window that has the same shape and orientation to select a subset of points from the same hypercubic lattice that project onto the same projection space. Their construction differs only in the position of the acceptance window in the direction orthogonal to the projection space.

On the other hand, one might think the degree of hyperuniformity *would* vary with LI class, with the following reasoning: Changing the decoration of the fundamental unit cell of crystals affects the degree of hyperuniformity. (This can be seen, e.g. with the triangular, kagome and honeycomb crystals

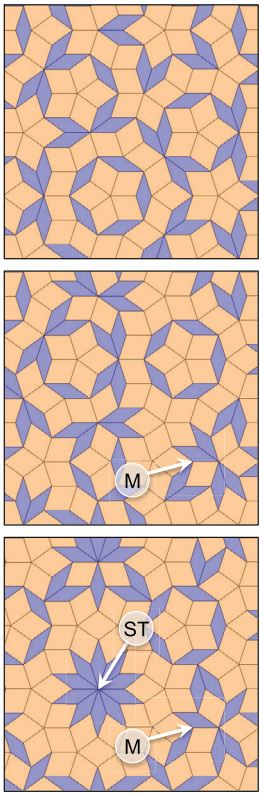

Figure 1. Tilings from three different LI classes. The Penrose tiling is shown at the top. From top to bottom, they correspond to $\gamma = 0$, $\gamma = 0.2$, and $\gamma = 0.5$. Though all are constructed from the same fat (orange) and skinny (violet) tiles, they differ in their distribution of vertex environments. The ST vertex is absent in the $\gamma = 0$ and $\gamma = 0.2$ LI classes. The M vertex is absent in the $\gamma = 0$ class. (See figure 4 for notation and enumeration of the sixteen distinct vertex environments.)

[5, 6].) Although different LI classes have identical fundamental repeating units (e.g. tiles in the case of quasicrystal tesselations) and identical Bragg peak positions, their diffraction patterns have different scattering intensities (similar to what occurs by changing the decoration of the unit cell in a crystal pattern). Also, with the direct projection method, while the acceptance window is the same for the different LI classes, when the hypercubic lattice points are projected into the space that includes the acceptance window, they are confined to planes that cut the acceptance window in different ways for different LI classes.

In this paper, we will provide clear evidence showing the latter intuition—that the degree of hyperuniformity varies with LI class—is correct. We will study a continuous set of LI classes of two-dimensional, pentagonal quasicrystal tilings, which can be obtained as duals to a multigrid composed of five overlapping sets of periodically spaced lines or as direct projections from a five-dimensional hypercubic lattice [3, 8, 9]. The set of tilings includes a continuum of configurations with five-fold symmetry and discrete instances with ten-fold symmetry, which includes the Penrose tiling [10]. Examples from different LI classes are shown in figure 1. In determining their degree of hyperuniformity, we will treat the quasicrystal tilings as point patterns, with points at the vertices of the tiles.

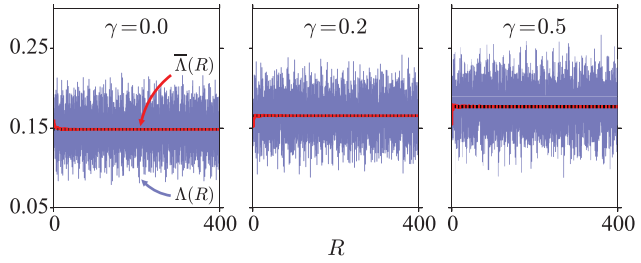

Figure 2. The small-scale function $\Lambda(R)$ (purple), running average $\overline{\Lambda}(R)$ (red), and global average $\overline{\Lambda}(\infty)$ (dashed black line), as defined in the text are shown, calculated for the three tilings in figure 1. The running average $\overline{\Lambda}(R)$ and the global average $\overline{\Lambda}(\infty)$ are indistinguishable for all but the smallest values of R. The small-scale function $\Lambda(R)$ appears to have bounded variations.

The notion of hyperuniformity can be formulated as follows: Given a point pattern in d-dimensional Euclidean space $\mathbb{R}^d$, we let $N(R;\mathbf{x}_0)$ be the number of points within a hyperspherical window of radius R with center at position $\mathbf{x}_0$, which is a random variable. For a fixed R, we let $\sigma^2(R) \equiv \langle N^2(R)\rangle - \langle N(R)\rangle^2$ be the number variance associated with this random variable. For typical disordered systems, $\sigma^2(R)$ asymptotically follows a volume law $\sigma^2(R) \sim R^d$. A system is said to be *hyperuniform* if $\sigma^2(R)$ grows more slowly than the volume of the window, i.e. $\sigma^2(R) \sim R^\alpha$ where $\alpha < d$. All ideal crystals and many quasicrystals are hyperuniform with $\alpha = d - 1$ [5, 6, 11], as are special disordered systems (a recent review of hyperuniform disordered systems can be found in [7]).

Our numerical results suggest that the particular quasicrystal tilings studied here are also hyperuniform with $\alpha = d - 1$, implying their local number variance has the asymptotic behavior [5, 6]

$$\sigma^2(R) \sim \Lambda(R)R + o(R), \tag{1}$$

where $\Lambda(R)$ is a bounded function that fluctuates around some average value, and $o(R)$ denotes terms of lower order than R. We therefore conjecture that the same holds for the entire continuous set of LI classes explored in this paper. It is useful to average out the small-scale variations in $\Lambda(R)$ and consider the running (cumulative moving) average $\overline{\Lambda}(R)$ [12] and the global average $\overline{\Lambda}(\infty)$ [5, 6], which are defined as follows:

$$\overline{\Lambda}(R) \equiv \frac{1}{R}\int_0^R \Lambda(R')\mathrm{d}R', \tag{2}$$

and

$$\overline{\Lambda}(\infty) \equiv \lim_{R\to\infty} \overline{\Lambda}(R). \tag{3}$$

In figure 2, we show $\Lambda(R)$ (purple), $\overline{\Lambda}(R)$ (red), and $\overline{\Lambda}(\infty)$ (black, dashed) for the three tilings in figure 1. Following [5] and [6], we shall use $\overline{\Lambda}(\infty)$ to characterize the *degree of hyperuniformity* of a given system.

In this paper, we will examine how $\overline{\Lambda}(\infty)$ varies with LI class and why. We begin in section 2 by describing how we construct quasicrystals and establishing some terminology. Section 3 details our numerical methods for determining $\overline{\Lambda}(\infty)$. Finally, in section 4, we present and discuss our main

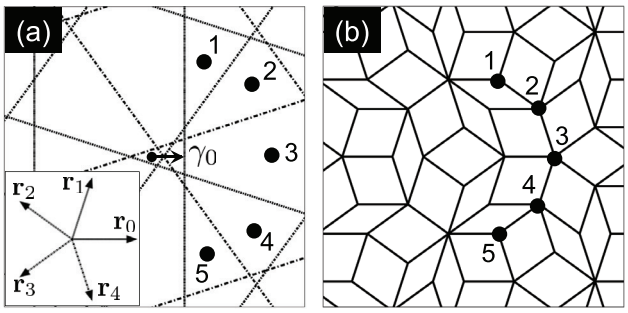

Figure 3. Schematic illustration of the dual method, as described in the text. (a) Periodic pentagrid, consisting of five grids (overlapping sets of periodically spaced lines), each normal to one of the five vectors $\mathbf{r}_i$ (inset). Each grid has been displaced from the origin by a finite phase γ_i. The extent of the 0th phase γ_0 is marked. Five open regions have been numbered. (b) Tiling obtained by applying the dual transformation to the pentagrid in (a). Vertices corresponding to the five numbered open regions in (a) are shown.

results, which show that $\overline{\Lambda}(\infty)$ varies continuously with the LI class, has a global minimum at the Penrose LI class, and has local minima at a special denumerable subset of LI classes known as *restorable* [13], which means, roughly, that they contain a lower variance in their local neighborhoods than do nearby LI classes. We also present empirical evidence indicating that the overall trend in $\overline{\Lambda}(\infty)$ can be attributable to the distribution of vertex environments.

2. Quasicrystals: dual method, local isomorphism, and restorability

In this section, we first describe how the two-dimensional pentagonal quasicrystals studied in this paper are generated via the 'dual method'. We establish that the LI classes can be continuously parameterized by a number γ and define the condition for when two LI classes are locally isomorphic. The notion of restorability is introduced, which will be useful to understand how $\overline{\Lambda}(\infty)$ varies with γ.

The quasicrystal tilings studied in this paper are the same as those generated by the 'direct projection method' using a rhombic-icosahedron acceptance window to select a subset of points from a five-dimensional hypercubic lattice that project onto a planar surface, forming the vertices of the tiling. Hence, the tilings are referred to as 'direct projection tilings' (DPTs) [13]. (Further details on both the direct projection method and the dual method can be found in [3, 8] and [9].)

The dual method is schematically illustrated in figure 3 and briefly reviewed here: A *periodic grid* is an infinite set of parallel, straight lines, with equal spacing between adjacent grid lines, labeled by $n \in \mathbb{Z}$ corresponding to their ordinal position in the grid. We take here the spacing between adjacent grid lines to be one. A *periodic pentagrid* (shown in figure 3(a)) comprises five periodic grids, with the ith grid oriented normal to the vector $\mathbf{r}_i = (\cos 2\pi i/5, \sin 2\pi i/5)$. The displacement γ_i of the ith grid from the origin is called the *phase*. The pentagrid partitions space into open regions, each of which can be uniquely labeled by a set of five integers $\mathbf{K} \equiv (k_0, k_1, \ldots, k_4)$ such that, if $\mathbf{x}$ is any point within the region, it lies between lines k_i and $k_i + 1$ of the ith grid. The dual method maps these open regions $\mathbf{K}$ to the vertices $\mathbf{t}$ of a tiling, according to the transformation $\mathbf{t} = \sum_{i=0}^{4} k_i \mathbf{r}_i$. Open regions that share an edge are mapped to vertices connected by an edge. The tilings so constructed comprise two rhombuses of equal sides but with angles of $2\pi/5$ ('fat') and $2\pi/10$ ('skinny'). For all DPTs, the ratio of the numbers of fat and skinny tiles equals $\tau = (1 + \sqrt{5})/2 \approx 1.618$, the golden ratio. Therefore, the corresponding point patterns, with points on the vertices, all have the same average number of points per unit area.

Two tilings are said to be *locally isomorphic* if any configuration of tiles in any finite region from one will occur with the same frequency in the other. It can be shown [3] that two tilings are locally isomorphic (up to inversion) if, and only if, the sum of the phases $\gamma \equiv \sum_{i=0}^{4} \gamma_i$, $\gamma' \equiv \sum_{i=0}^{4} \gamma_i'$ are related by

$$\left| -\frac{1}{2} + \{\gamma\} \right| = \left| -\frac{1}{2} + \{\gamma'\} \right| \tag{4}$$

where $\{\gamma\}$ denotes the fractional part of γ. An arbitrary γ can be mapped to a locally isomorphic γ' that lies within the range [0,0.5] via

$$\gamma' = \frac{1}{2} - \left| -\frac{1}{2} + \{\gamma\} \right|. \tag{5}$$

If $\gamma, \gamma' \in [0, 0.5]$ and $\gamma \neq \gamma'$, then γ, γ' are not locally isomorphic.

To understand how $\overline{\Lambda}(\infty)$ varies with γ, it will be useful to characterize the tile configurations of the different LI classes. For this, we shall employ the concepts of r-maps and r-atlases: Given a tiling, select a vertex and construct a circle of radius r centered at that vertex. The collection of all tiles that are entirely contained within the circle is called an r-map. Repeat this for every vertex in the tiling. The resulting collection of r-maps is called the r-atlas for that tiling (taking out duplicates and configurations equivalent under reflections and rotations).

An LI class is said to be *restorable* if there is some finite R_r, called the *restorability radius*, such that the R_r-atlas is unique to that LI class, among all DPTs. A restorable LI class γ with restorability radius R_r has the property that its R_r-atlas contains the fewest number of R_r-maps, compared to LI classes with $\gamma' = \gamma \pm \delta\gamma$, in the limit $\delta\gamma \to 0$. For DPTs, it has been shown that the only restorable LI classes are those with $\gamma = n\tau$, where $n \in \mathbb{Z}$ and $\tau = (1 + \sqrt{5})/2 \approx 1.618$ is the golden ratio [13]. For the $\gamma = n\tau$ class, R_r is proportional to n. That is, as n increases, one must consider all tile configurations out to larger and larger sizes to distinguish the $\gamma = n\tau$ class from all other LI classes.

Also useful in our discussion of how $\overline{\Lambda}(\infty)$ varies with γ is the notion of vertex environments. A *vertex environment* is defined to be a collection of tiles sharing a common vertex. Up to rotations and reflections, there are sixteen distinct vertex environments (shown in figure 4) that can be constructed from the skinny and fat rhombuses. Each LI class has a characteristic distribution of vertex environments [14–16]. The distribution of vertex environments for the different LI classes is shown in figure 5.

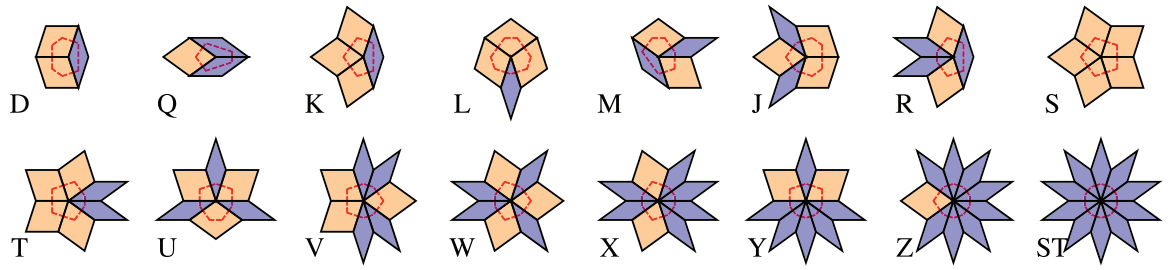

Figure 4. The sixteen distinct vertex environments, constructed from fat (orange) and skinny (violet) tiles. The Voronoi areas are outlined in dashed, red lines. Notation follows that of [8, 9] and [14].

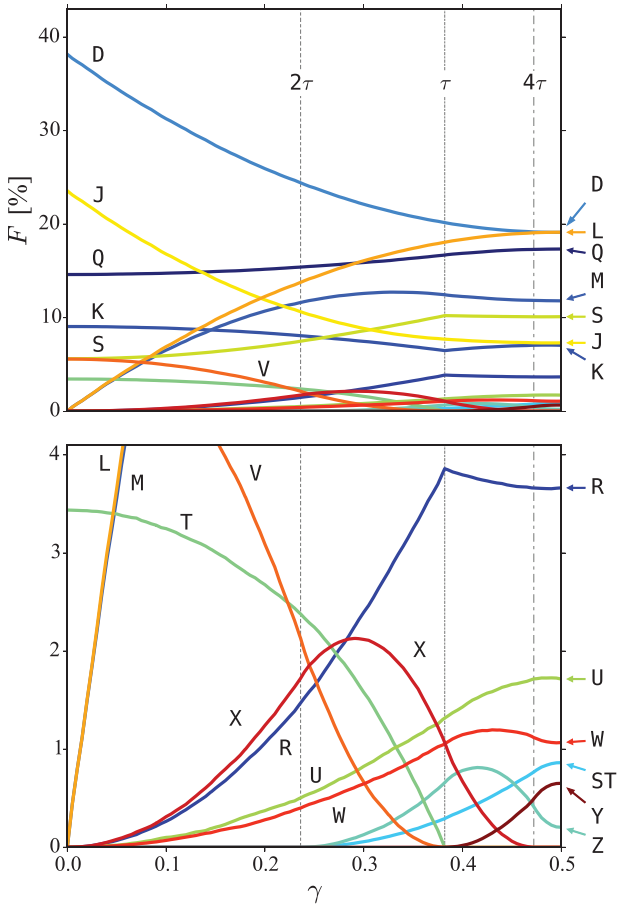

Figure 5. Frequencies F of the sixteen vertex environments, which are shown in figure 4, versus LI class γ. The lower portion of the top panel is magnified in the bottom panel. Dashed vertical lines mark $\gamma \approx 0.236, 0.382, 0.472$, which correspond to $\gamma = 2\tau, \tau, 4\tau$; at these values of γ (and at $\gamma = 0$), certain vertex environments appear or disappear. Frequencies were calculated in [15] but have been independently re-calculated here.

Among all restorable LI classes, the Penrose LI class ($\gamma = 0$) has the smallest restorability radius. It is also distinguished for having the fewest distinct vertex environments.

3. Determining $\overline{\Lambda}(\infty)$

In this section, we describe how we numerically estimate the degree of hyperuniformity $\overline{\Lambda}(\infty)$, defined by (3), for the different LI classes.

We first generate a DPT from LI class γ using the dual method. This is necessarily a finite portion of the perfect, infinite tiling and is not a periodic approximant. Treating the tilings as point patterns, with points at the vertices of the tiles, we estimate the local number variance $\sigma^2(R)$ by, first, counting the number of points $N(R; \mathbf{x}_i)$ lying within M circular sampling windows of radius R with centers at positions $\mathbf{x}_i$ ($i = 1, \ldots, M$), then calculating the variance in these counts as follows:

$$\sigma^2(R) = \frac{1}{M}\sum_{i=1}^{M} N(R; \mathbf{x}_i)^2 - \frac{1}{M^2}\left(\sum_{i=1}^{M} N(R; \mathbf{x}_i)\right)^2. \qquad (6)$$

This is repeated for a set of radii R_i, uniformly distributed between $R_{\min}$ and $R_{\max}$.

The window centers $\mathbf{x}_i$ are uniformly distributed within a circular region of radius $R_{\max}$ about the center of mass of the quasicrystal point pattern. The fiducial area, which contains all points that can be sampled, is a circular region about the center of mass of radius $2R_{\max}$. The DPT must be sufficiently large to contain within its boundaries this fiducial area. (We have found that a sufficiently large DPT can be generated from a pentagrid containing $2R_{\max}/a$ grid lines per grid.)

We calculate the running average $\overline{\Lambda}(R)$ by using a trapezoidal rule to numerically integrate (2) up to $R_{\max}$:

$$\overline{\Lambda}(R_i) \equiv \frac{1}{R_i - R_{\min}} \sum_{j=2}^{i} \frac{\lambda_{j-1} + \lambda_j}{2} \Delta R_j, \qquad (7)$$

where $\lambda_j \equiv \sigma^2(R_j)/R_j$ and $\Delta R_j \equiv R_j - R_{j-1}$. Our estimate of the global average $\overline{\Lambda}(\infty)$ is obtained by fitting $\overline{\Lambda}(R_i)$ to the two-parameter curve

$$\overline{\Lambda}(R) = \overline{\Lambda}(\infty) + C/R \qquad (8)$$

where C is a second free parameter. (Using an F-test and a comparison of residual sum of squares, we determined that the C/R subleading term is a better fit than (i) no subleading term ($C = 0$), (ii) a subleading term $C\log(R)/R$, and (iii) a subleading term C/R^2.)

As a test of our procedure, we evaluate $\overline{\Lambda}(\infty)$, varying the upper integration limit $R_{\max}$, for different crystal point patterns: kagome, honeycomb, square, and triangle lattices. The lattice spacings have been chosen so that the number of points per unit area is one. For each crystal point pattern, the window centers are chosen to be uniformly distributed within the unit cell. These estimates are shown in figure 6, with the ideal values computed in [5] and [6] overlaid in dashed lines. Our

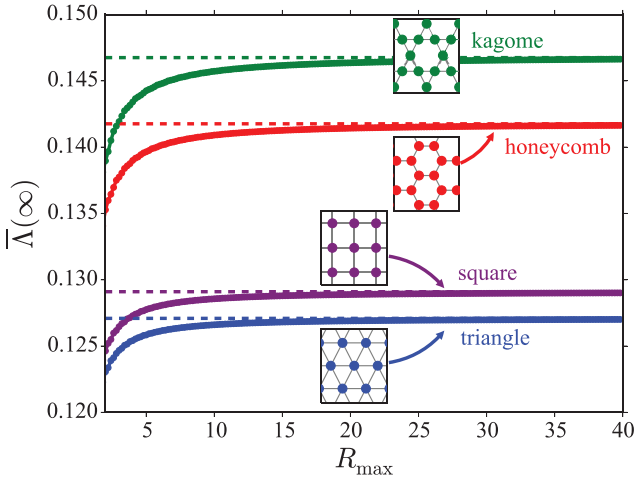

Figure 6. Estimates of the degree of hyperuniformity $\overline{\Lambda}(\infty)$, as the upper integration limit $R_{\max}$ is varied, for kagome, honeycomb, square, and triangle crystal point patterns. The ideal values are overlaid in dashed lines (from [5] and [6]).

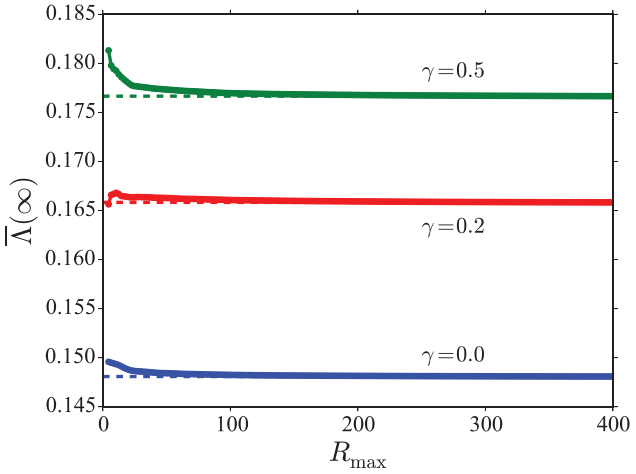

Figure 7. Estimates of the degree of hyperuniformity $\overline{\Lambda}(\infty)$, as the upper integration limit $R_{\max}$ is varied, for three quasicrystal point patterns. Portions of the corresponding tilings are shown in figure 1. Estimates of $\overline{\Lambda}(\infty)$ evaluated at $R_{\max} = 400$ are overlaid in dashed lines.

procedure approaches an accuracy that is within 0.1% of the ideal values for $R_{\max} \gtrsim 27$ for the triangle and square lattices and $R_{\max} \gtrsim 35$ for the honeycomb and kagome crystals.

We perform a similar test with the quasicrystal point patterns. In figure 7, we show, for three representative LI classes, our estimates of $\overline{\Lambda}(\infty)$ as the upper integration limit $R_{\max}$ is varied. Comparing with $\overline{\Lambda}(\infty)$ evaluated at $R_{\max} = 400$ (dashed lines), the percentage difference is less than 0.1% for $R_{\max} \gtrsim 100$ for the $\gamma = 0$ class and $R_{\max} \gtrsim 150$ for $\gamma = 0.2$ and $\gamma = 0.5$. We also tested how $\overline{\Lambda}(\infty)$ varies with the number of windows M and found that, comparing with $M = 10\,000$, the percentage difference is less than 0.1% for $M \gtrsim 3500$.

For the estimates of $\overline{\Lambda}(\infty)$ presented in this paper, we used the conservative choices of $R_{\max} = 400$ and $M = 10\,000$. Moreover, the sampling of LI classes γ must be treated with care, because random sampling would miss features that occur at the discrete set of points $\gamma = n\tau$. We do a uniform sampling from 0 to 0.5 in intervals of 0.005, in addition to sampling $n\tau$ for n from 1 to 15. The values of γ are mapped to equivalent values lying within the interval [0,0.5] using (5).

4. Results and discussion

Our calculation of $\overline{\Lambda}(\infty)$ versus γ for pentagonal DPTs is shown in figure 8. There are noteworthy features in $\overline{\Lambda}(\infty)$, as a function of γ, that may not have been expected. The function appears to be continuous and increases on average. It also appears to have a global minimum at the Penrose LI class ($\gamma = 0$), a global maximum at $\gamma = 0.5$, and local minima at the restorable LI classes ($\gamma = n\tau$). The local minima are cusplike, not smooth. Moreover, the depths of these local minima appear to decrease with respect to n. In figure 8, we have included a magnified portion of the curve around $\gamma = \tau$, where a finer resolution sampling of γ was performed.

As shown in the upper panel of figure 9, the increasing trend of $\overline{\Lambda}(\infty)$ with γ is already exhibited by $R_{\max} = 2$. This indicates that the trend must be attributable to local geometrical features on length scales of order $\leqslant 2$, given that this estimate of $\overline{\Lambda}(\infty)$ was obtained from information contained in sampling windows with radius $\leqslant 2$. As shown in the lower panel, by $R_{\max} = 16$, the cusp at $n = 1$ begins to appear, with more cusps appearing as $R_{\max}$ increases.

To explore the dependence of $\overline{\Lambda}(\infty)$ on the local geometry of the DPTs, we construct their Voronoi tesselations, considering the vertices as a point pattern. The *Voronoi cell* of a vertex is the region of space within which all points in space are closer to that vertex than to any other. Each of the sixteen vertex environments in figure 4 has a corresponding Voronoi cell (shown in figure 4 as dashed, red lines), with an area that we denote by A_i ($i = 1, \ldots, 16$). The tesselation of space by the Voronoi cells is the *Voronoi tesselation*. The distribution of Voronoi cell areas in the Voronoi tesselation quantifies the local geometric structure of the point pattern.

We compute the standard deviation σ_V of the Voronoi cell areas as follows:

$$\sigma_V \equiv \sqrt{\sum_{i=1}^{16} F_i (A_i - \mu_V)^2}\,, \tag{9}$$

where we have used the frequencies F_i of the vertex environments from figure 5, and $\mu_V \equiv \sum_{i=1}^{16} F_i A_i$ is the average Voronoi cell area. The normalized standard deviation σ_V/μ_V of the areas is shown in figure 10 as a function of γ. We observe that the distribution of vertex environments, as characterized by σ_V/μ_V, is monotonic with γ and increases with γ in a manner similar to $\overline{\Lambda}(\infty)$ in figure 8, excluding the cusps.

We therefore see two competing effects: the local ordering (e.g. as measured by σ_V/μ_V) and the restorability (e.g. as measured by the restorability radius R_r). The restorability radius is a characteristic length scale of the restorable LI classes. It is smallest for the Penrose LI class, which has the highest degree of hyperuniformity, so one might have expected $\overline{\Lambda}(\infty)$ to grow monotonically with R_r. Instead, we claim that the leading effect is the local ordering, which is monotonic with γ. The

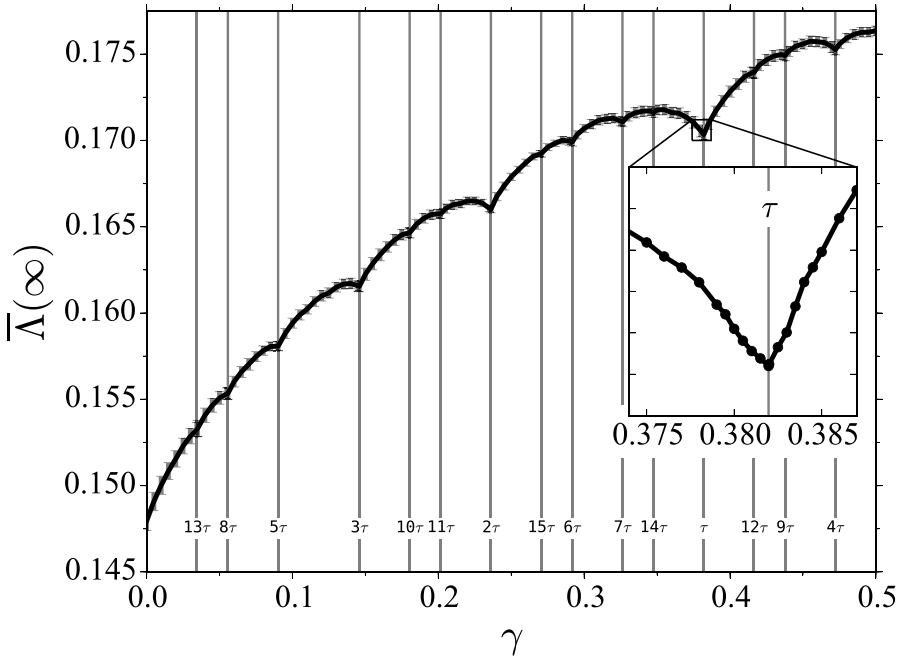

Figure 8. Degree of hyperuniformity $\overline{\Lambda}(\infty)$ versus LI class γ. The vertical lines mark the restorable LI classes $\gamma = \tau, 2\tau, \ldots, 15\tau$, mapped to equivalent values lying within the interval [0, 0.5] using (5). Magnified portion around $\gamma = \tau$ shows the typical structure of the local minima. Each point represents an average over ten tilings from the same LI class γ. The error bars represent the standard deviation of the estimates of $\overline{\Lambda}(\infty)$. Pentagrids contain 800 grid lines per grid; each tiling contains approximately 3.5×10^6 vertices; upper integration limit $R_{\max} = 400$ and number of windows $M = 10\,000$.

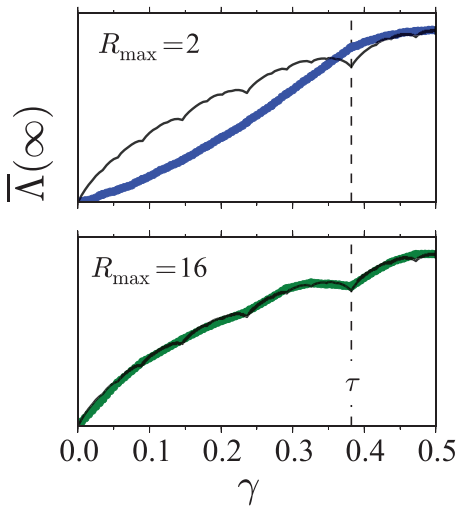

Figure 9. Degree of hyperuniformity $\overline{\Lambda}(\infty)$ evaluated at $R_{\max} = 2$ (blue, upper panel) and 16 (green, lower panel), overlaid on the curve from figure 8, which was evaluated at $R_{\max} = 400$. The curves have been rescaled so that $\overline{\Lambda}(\infty)$ at $\gamma = 0$ and at $\gamma = 0.5$ are set to 0 and 1, respectively. The dashed vertical line at $\gamma \approx 0.382$ marks the $\gamma = \tau$ class.

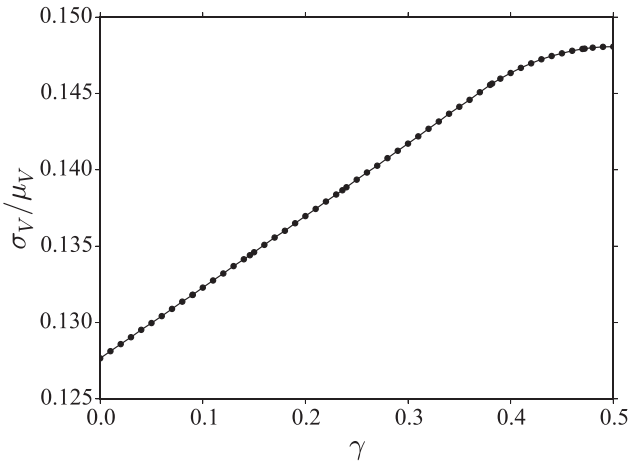

Figure 10. Normalized standard deviation σ_V/μ_V of the Voronoi cell areas versus LI class γ.

deviations from monotonicity with γ (i.e. the depths of the cusps) are a subdominant effect that is monotonic with the restorability radius. The evidence that the local ordering is the dominant factor in determining the degree of hyperuniformity is that the value of $\overline{\Lambda}(\infty)$ is not monotonic in R_r, but, instead, is more correlated with γ.

As noted in the Introduction, it had been an open question whether the degree of hyperuniformity varies with LI class. The results above clearly show the answer is yes. Evidently, the repeating units and the symmetry do not, by themselves, determine the degree of hyperuniformity—the continuum of DPTs studied here are constructed from the same tiles and have the same five-fold symmetry (with the exceptions of $\gamma = 0$ and $\gamma = 0.5$, which have ten-fold symmetry, although the tilings corresponding to these two special choices of γ also have different values of $\overline{\Lambda}(\infty)$). The results also show, for the DPTs studied here, that the differences in hyperuniformity are largely attributable to local differences in point (or tile)

configurations and that restorability plays a factor. Our initial studies using other tile decorations show qualitatively similar results.

A primary question of interest is whether the differing degree of hyperuniformity among LI classes has any physical consequence, such as on electronic and photonic transport properties. This will be the subject of future study.

Acknowledgments

We thank the anonymous reviewers for their valuable suggestions and comments, which led to improvements of the manuscript. CL thanks Duyu Chen, JaeUk Kim, and Ge Zhang for helpful discussions during the early stages of this work. We express our gratitude to James Earle Fraser for continued inspiration.

References

[1] Levine D and Steinhardt P J 1984 Quasicrystals: a new class of ordered structures *Phys. Rev. Lett.* **53** 2477–80
[2] Levine D and Steinhardt P J 1986 Quasicrystals. I. Definition and structure *Phys. Rev.* B **34** 596–616
[3] Socolar J E S and Steinhardt P J 1986 Quasicrystals. II. Unit-cell configurations *Phys. Rev.* B **34** 617–47
[4] Steinhardt P J and DiVincenzo D P 1999 Quasicrystals: the state of the art *Directions in Condensed Matter Physics* 2nd edn (Singapore: World Scientific)
[5] Torquato S and Stillinger F H 2003 Local density fluctuations, hyperuniformity, and order metrics *Phys. Rev.* E **68** 041113
[6] Zachary C E and Torquato S 2009 Hyperuniformity in point patterns and two-phase random heterogeneous media *J. Stat. Mech.* P12015
[7] Torquato S 2016 Hyperuniformity and its generalizations *Phys. Rev.* E **94** 022122
[8] de Bruijn N G 1981 Algebraic theory of Penrose's non-periodic tilings of the plane. I *Indagationes Math.* **84** 39–52
[9] de Bruijn N G 1981 Algebraic theory of Penrose's non-periodic tilings of the plane. II *Indagationes Math.* **84** 53–66
[10] Penrose R 1974 The rôle of aesthetics in pure and applied mathematical research *Inst. Math. Appl. Bull.* **10** 266–71
[11] Oğuz E C, Socolar J E S, Steinhardt P J and Torquato S 2017 Hyperuniformity of quasicrystals *Phys. Rev.* B **95** 054119
[12] Kim J and Torquato S 2017 Effect of window shape on the detection of hyperuniformity via the local number variance *J. Stat. Mech.* 013402
[13] Ingersent K and Steinhardt P J 1990 Matching rules and growth rules for pentagonal quasicrystal tilings *Phys. Rev. Lett.* **64** 2034–7
[14] Pavlovitch A and Kléman M 1987 Generalised 2D Penrose tilings: structural properties *J. Phys. A: Math. Gen.* **20** 687–702
[15] Zobetz E and Preisinger A 1990 Vertex frequencies in generalized Penrose patterns *Acta Crystallogr.* A **46** 962–70
[16] Henley C L 1986 Sphere packings and local environments in Penrose tilings *Phys. Rev.* B **34** 797–816